HIPPOCAMPUS 22:2276–2289 (2012)

CaMKII, MAPK, and CREB are Coactivated in Identified Neurons in a Neocortical Circuit Required for Performing Visual Shape Discriminations

Guo-Rong Zhang,[1] Hua Zhao,[1] Eui M. Choi,[1] Michael Svestka,[1] Xiaodan Wang,[1] Robert G. Cook,[2] and Alfred I. Geller[1]*

ABSTRACT: Current theories postulate that the essential information for specific cognitive tasks is widely dispersed in multiple forebrain areas. Nonetheless, synaptic plasticity and neural network theories hypothesize that activation of specific signaling pathways, in specific neurons, modifies synaptic strengths, thereby encoding essential information for performance in localized circuits. Consistent with these latter theories, we have shown that gene transfer of a constitutively active protein kinase C into several hundred glutamatergic and GABAergic neurons in rat postrhinal cortex enhances choice accuracy in visual shape discriminations, and the genetically-modified circuit encodes some of the essential information for performance. However, little is known about the role of specific signaling pathways required for learning, in specific neurons within a critical circuit. Here we show that three learning-associated signaling pathways are coactivated in the transduced neurons during both learning and performance. After gene transfer, but before learning a new discrimination, the calcium/calmodulin-dependent protein kinase (CaMKII), MAP kinase, and CREB pathways were inactive. During learning, these three pathways were coactivated in the transduced neurons. During later performance of the discrimination, CaMKII activity declined, but MAP kinase and CREB activity persisted. Because the transduced neurons are part of a circuit that encodes essential information for performance, activation of these learning-associated signaling pathways, in these identified neurons, is likely important for both learning and performance. © **2012 Wiley Periodicals, Inc.**

KEY WORDS: visual learning; postrhinal cortex; signaling pathways; synaptic plasticity; protein kinase C

INTRODUCTION

Current theories postulate that the essential information for specific cognitive tasks is encoded in multiple forebrain areas, in a distributed network, although the specific critical areas and encoding mechanisms remain contentious (McClelland et al., 1995; Squire and Alvarez, 1995; Nadel and Moscovitch, 1997; Moser and Moser, 1998; Dudai, 2004; Frankland and Bontempi, 2005). Nonetheless, synaptic plasticity and neural network theories hypothesize that activation of specific signaling pathways, in specific neocortical neurons, modifies synaptic strengths, thereby encoding the essential information for performance in localized circuits (Rumelhart et al., 1986; Dudai, 1989). Specific learning-associated signaling pathways include the calcium/calmodulin-dependent protein kinase II (CaMKII), MAP kinase, and CREB pathways (Silva et al., 1992, 1998; Bozon et al., 2003; Elgersma et al., 2004; Sweatt, 2004; Wayman et al., 2008). However, we have limited knowledge about which specific signaling pathways are activated during learning or performance, in identified neurons, that are part of a neocortical circuit required for learning.

To enable studies on learning-associated signaling in a critical circuit, we genetically-modified a circuit in rat postrhinal (POR) cortex to encode some of the essential information for performing specific visual shape discriminations (Zhang et al., 2005, 2010a). Specifically, we activated protein kinase C (PKC) pathways in small groups of POR cortex neurons before visual discrimination learning. We performed gene transfer into POR cortex because it is required for this learning (Winters et al., 2004; Murray et al., 2007). Further, POR cortex and perirhinal cortex have large reciprocal connections (Burwell and Amaral, 1998), and many of the transduced neurons in POR cortex project to perirhinal cortex (Zhang et al., 2010b); thus, the transduced neurons in POR cortex may also affect perirhinal cortex physiology. We activated PKC pathways because specific PKC genes are required for multiple types of learning (Abeliovich et al., 1993; Weeber et al., 2000). Further, a constitutively active, catalytic domain of PKCζ is necessary for hippocampal long-term potentiation (LTP) (Ling et al., 2002), spatial learning (Pastalkova et al., 2006), and insular cortex-mediated taste learning (Shema et al., 2007). The constitutively active PKC used here is a catalytic domain of PKCßII (Song et al., 1998), and all the PKC catalytic domains are homologous (Hanks et al., 1988). Delivery of a constitutively active PKC into several hundred spatially grouped glutamatergic and GABAergic neurons in POR cortex (via a virus vector), activated PKC pathways, increased

[1] **Department of Neurology, W. Roxbury VA Hospital/Harvard Medical School, W. Roxbury, Massachusetts;** [2] **Department of Psychology, Tufts University, Medford, Massachusetts**

Additional Supporting Information may be found in the online version of this article.

Grant sponsor: NIH; Grant numbers: AG025894 (to G.-R.Z.); NS045855 (to A.I.G.); NS057558 (to A.I.G.); Grant sponsor: NSF (to R.G.C.)

*Correspondence to: Alfred Geller, W. Roxbury VA Hospital/Harvard Medical School, 1400 VFW Parkway, W. Roxbury, MA 02132, USA.
E-mail: alfred_geller@hms.harvard.edu

Accepted for publication 25 May 2012
DOI 10.1002/hipo.22045
Published online 27 June 2012 in Wiley Online Library (wileyonlinelibrary.com).

activation-dependent neurotransmitter release, and supported both faster learning and improved steady state accuracy in subsequent visual shape discriminations (Song et al., 1998; Cook et al., 2004; Zhang et al., 2005). Further, after both the gene transfer and the learning, creation of small neurochemical lesions proximal to the gene transfer site selectively reduced performance only for discriminations learned after gene transfer; these lesions ablated ~21% of POR cortex, including most of the transduced neurons (Zhang et al., 2010a). Thus, the genetically-modified circuit, which contains the transduced neurons, encodes some of the essential information for performance. Correlatively, activity-dependent gene imaging confirmed increased activity in the genetically-modified circuit during performance, and showed the essential circuit contains ~500 neurons and is sparse-coded (Zhang et al., 2005, 2010a). Wild-type (wt) rats contain similar circuits, but at different, unpredictable positions among the rats (Zhang et al., 2010a), suggesting that similar encoding mechanisms exist in wt rats. [This introductory information is detailed in Zhang et al. (2005, 2010a) and the Supporting information for Zhang et al. (2010a).]

Here we show that during learning and performance of a new visual discrimination, specific learning-associated signaling pathways are activated in the identified, transduced neurons within this essential neocortical circuit. After gene transfer but before learning, the CaMKII, MAP kinase, and CREB pathways exhibited minimal activity in the transduced neurons. During subsequent learning, each of these pathways exhibited increased levels of activity, in both experimental and control groups. Importantly, the experimental condition, constitutively active PKC and learning a new image set, supported higher levels of activity in each pathway than the learning control groups. After learning reached steady-state levels, CaMKII pathway activity declined, whereas the MAP kinase and CREB pathways remained activated at levels similar to those observed during initial learning. Correlatively, we confirmed previous results (Zhang et al., 2005) that the constitutively active PKC increases accuracy for learning and performing new visual discriminations. In summary, these results identify three learning-associated signaling pathways that are activated during cognitive learning, in identified neurons in an essential circuit for performance.

MATERIALS AND METHODS

Vectors and Packaging

pINS-TH-NFHpkcΔ\INS-TH-NFHlac (PkcΔ vector) and pINS-TH-NFHpkcΔGG\INS-TH-NFHlac (PkcΔGG vector) have been described (Wang et al., 2001; Zhang et al., 2005). pkcΔ contains the catalytic domain of rat PKCβII (nucleotide 994 to the 3′ end), and the flag tag fused to the 5′ terminus of this catalytic domain (Song et al., 1998). In PkcΔGG, an absolutely conserved lys, required for phosphoryl transfer, was replaced with a gly (Hanks et al., 1988; Song et al., 1998). PkcΔ exhibits a substrate specificity similar to rat brain PKC, and PkcΔGG lacks protein kinase activity (Song et al., 1998). Each vector contains two transcription units; one transcription unit expresses either PkcΔ or PkcΔGG, and the second transcription unit expresses ß-galactosidase (ß-gal), a histological marker. Each transcription unit uses a modified neurofilament promoter, which contains, 5′ to 3′, the chicken ß-globin insulator (INS; 1.2 kb), an enhancer from the rat tyrosine hydroxylase promoter (TH; −0.5 kb to −6.8 kb), and a mouse neurofilament heavy gene promoter (NFH; 0.6 kb) (Zhang et al., 2000). The INS-TH-NFH promoter supports expression in forebrain neurons for 6 or 14 months, the longest times examined, and time courses in the striatum and hippocampus showed expression in similar numbers of cells at times similar to the beginning or end of visual testing (Zhang et al., 2000; Sun et al., 2004).

Helper virus-free Herpes Simplex Virus (HSV-1) vector packaging, purification, and titering were performed as described (Fraefel et al., 1996; Lim et al., 1996; Sun et al., 1999) (titers, $5.0 \pm 0.1 \times 10^6$ (mean ± SEM) infectious vector particles/ml). For each experiment, the titers of the different stocks were matched by dilution. No HSV-1 (<10 pfu/ml) was detected in these stocks. This helper virus-free HSV-1 vector system causes minimal side effects [Fraefel et al., 1996; Zhang et al., 2005; see Supporting Information text in Zhang et al. (2010a)].

Visual Testing Apparatus

Twelve operant chambers were used for testing (Cook et al., 2004). Each computer-controlled apparatus was placed in a box (FIS units, Plas Labs) containing an overhead fluorescent light and speaker. A ventilation fan on the rear panel also provided masking white noise. An infrared touchscreen (IRFP-10.4, Elotouch Systems) was mounted in the center of one of the long sides of a clear plastic rat cage (46 L × 20 H × 24 D cm) and placed in front of a computer monitor. A central lever (ENV-110, Med. Associates) was located on the wall opposite the monitor, and a liquid feeder (ENV-110 and ENV-201A, Med. Associates) was located above the lever. A blind code identified the rats to both the computer and the computer operator throughout the experiment. For additional details, see (Cook et al., 2004) methods.

Simultaneous Two Object Visual Discrimination Testing

The rats started each trial by pressing the lever. This caused two images to appear on the monitor. The right/left location of these images was counterbalanced over blocks of 20 presentations and pseudo-randomly varied within a block with no more than three consecutive presentations on a side. When a rat made contact with the correct stimulus on the touchscreen, the speaker produced a 1-s sound and the feeder provided a 0.1-s milk reward (after four consecutive correct responses, the reward amount was doubled until an error). After an incorrect response, a large solid rectangle (23.5 × 10.1 cm) was flashed

on the monitor three times and the overhead houselight was turned off for 15 s. A correction procedure was used with every fourth incorrect response causing that trial to be presented again. Each session contained 120 discrimination trials or lasted 1 h. The rats were trained 7 days a week, 1 session per day. Three image sets were tested; each contained two objects of the same size: ⩵ vs. ||, seven alternating white and black bars, each one 1.6 (all lengths in cm) wide and 9.5 long; [] vs. +, [] 6.7 external side × 0.6 wide; +, 6.4 × 1.3 for each bar; / and \, 8.3 × 1.0 (45° or 135° for long side) (Cook et al., 2004; Zhang et al., 2005). Male Long Evans rats (initially ~6 weeks old; Charles River) were maintained on moderate food deprivation except during the surgery period, when food was available ad libitum. Water was available ad libitum. Experiments were approved by the VA Boston Healthcare System IACUC.

Gene Transfer

Vector stocks were delivered into the rats by stereotactic injection (two sites, 1/hemisphere, 3 μl/site) into POR cortex (anterior-posterior (AP) −8.0, medial-lateral (ML) ±6.0, dorsal-ventral (DV) −5.2) (Zhang et al., 2005). AP is relative to bregma, ML is relative to the sagittal suture, and DV is relative to the bregma-lambda plane (Paxinos and Watson, 1986). A micropump (Model 100, KD Scientific) was used for all injections. Vector stocks were injected over 5 min, and after 5 additional min, the 33 gauge needle was slowly retracted.

These injection conditions support gene transfer into several hundred spatially grouped cells in POR cortex (Zhang et al., 2005). Of note, >90% of the transduced cells are neurons, 52% are glutamatergic and 45% are GABAergic neurons, <1% are cholinergic, and no catecholaminergic neurons are observed. Of note, both glutamatergic or GABAergic neurons are typically activated during performance of a specific task; for example, activity-dependent gene imaging showed increased activity in both glutamatergic and GABAergic neurons in cat primary visual cortex following sensory/light stimulation (Van der Gucht et al., 2002, 2005). Further, the majority of the gene transfer is into neurons in POR cortex; specific neocortical areas with large projections to POR cortex, such as perirhinal cortex, contain <1% of the number of transduced neurons as POR cortex, and no transduced neurons were observed in specific subcortical areas, including the hippocampus, amygdala, specific cholinergic basal forebrain areas, and specific catecholaminergic midbrain areas (Zhang et al., 2005).

Delivery of the PkcΔ vector into POR cortex activated PKC pathways. PkcΔ increased phosphorylation of five PKC substrates, two receptors essential for glutamatergic neurotransmission and learning (AMPA receptor GluR2 subunit-Ser880-P, NMDA receptor NR-1 subunit-Ser896-P), a signal transduction protein (MARCKS-Ser159/163-P), and two proteins that have critical roles in neurotransmitter release (GAP-43-Ser41-P, Dynamin-Ser795-P) (Zhang et al., 2005). Further, PkcΔ supported activation-dependent increases in neurotransmitter release; PkcΔ increased release of dopamine and norepinephrine from cultured sympathetic neurons (Song et al., 1998), and glutamate and GABA from cultured temporal cortex cells (Zhang et al., 2005). Moreover, this intervention also increased both the learning rate and the steady-state accuracy for moderately difficult image sets ([] vs. + or / vs. \) ((Zhang et al., 2005) and this study).

Delivery of PkcΔ into specific brain areas and specific PKC knockout mice differ in four critical properties, and support different changes in learning. First, enzyme activity: PkcΔ is constitutively active, but a knockout mouse deletes a specific PKC gene. Second, affected neurons: PkcΔ-gene transfer affects small numbers of neurons in a specific area, but each PKC knockout mouse abolishes expression throughout the animal. Third, subcellular location: PkcΔ lacks a regulatory domain that targets specific PKC proteins to specific subcellular locations (Tanaka and Nishizuka, 1994). Fourth, protein levels: PkcΔ is expressed from a heterologous promoter (Zhang et al., 2000), removing feedback regulation of PkcΔ levels, but PKC genes undergo feedback regulation by their promoters. Of note, delivering PkcΔ into four different brain areas causes different changes in learning or behavior (Song et al., 1998; Neill et al., 2001; Oh et al., 2003; Zhang et al., 2005, 2010a). In contrast, PKCß or PKCγ knockout mice display deficits in fear conditioning (Weeber et al., 2000) or specific learning paradigms (Abeliovich et al., 1993), respectively. These different behavioral changes from PkcΔ or specific PKC knockout mice are due to the differences between the interventions.

Experimental Design

The initial training to familiarize the rats with the apparatus was performed as previously described (Cook et al., 2004). The rats were then trained on a control, pre-gene-transfer image set (⩵ vs. ||). Any difference in learning ability among rats was controlled by grouping the rats into sets of two based on the order in which they learned the discrimination and reached gene transfer; one rat received PkcΔ and the other received the control vector, PkcΔGG. After gene transfer, the rats were retested on ⩵ vs. ||, then trained on an experimental, new, post-gene-transfer image set ([] vs. +) for 1, 4, or 10 sessions, and then sacrificed. For CaMKII assays, rats were sacrificed 15 min after their last session, while for MAP kinase or CREB assays, rats were sacrificed 30 min after their last session (maximum phosphorylation levels were observed at these time points). Another control group received PkcΔ followed by retesting for 10 sessions on the pre-gene-transfer image set (⩵ vs. ||). Additional control groups received either PkcΔ or PkcΔGG, but no visual testing. These rats were sacrificed at 10 days after gene transfer. For the experiments to show enhanced learning, after gene transfer the rats were retested on the pre-gene-transfer image set, and then tested sequentially on / vs. \ and then [] vs. + for 10 sessions each.

Histological Analyses

Perfusion with paraformaldehyde, preparation of 25 μm coronal sections, and immunohistochemistry were performed as described (Zhang et al., 2005). The primary antibodies were

mouse monoclonal anti-flag (1:500 dilution; Sigma), rabbit anti-CaMKII-Thr286-P, rabbit anti-MAP Kinase-Thr202/Tyr204-P, or rabbit anti-CREB-Ser133-P (all 1:100 dilution; Cell Signaling Technology, Inc). Sections were mounted in PBS, and immediately examined under the microscope.

Costaining was quantified by obtaining digital images of each field with fluorescein or rhodamine filters (60× magnification), merging the images, and scoring all the transduced cells in each field that was analyzed; each field was scored at least twice, and the results differed by ≤10%. Sections from three to seven rats were examined for each vector, session, and phospho-specific antibody; except only two rats were examined for the PkcΔ, session 4, phospho-CREB condition. An average of 245 ± 13 (mean ± SEM) transduced cells were scored per rat for each condition (counts for each rat and condition are in Supporting Information Tables S1–S3).

Statistical Analyses

Statistical analyses were conducted using between groups or repeated measures ANOVAs (Sigmastat, SPSS Inc.).

RESULTS

After Gene Transfer but Before Learning, Transduced Neurons Exhibit Minimal Learning-Associated Signaling Activity

To examine learning-associated signaling in the transduced neurons, we chose to study three signaling pathways required for cognitive learning, the CaMKII, MAP kinase, and CREB pathways (Silva et al., 1992, 1998; Bozon et al., 2003; Elgersma et al., 2004; Sweatt, 2004; Wayman et al., 2008). For a syntax convention, we refer to each of these three pathways individually, as each pathway can function independent of the other two; however, we recognize that a specific pathway can activate another pathway (in particular, MAPK can activate CREB), and, thus, these pathways can also be viewed as earlier or later steps in the same pathway. The first experiment determined the activity of these pathways after gene transfer, but before learning. Gene transfer used our established conditions to deliver either a constitutively active PKC (PkcΔ) (Zhang et al., 2005), or a control (PkcΔGG, a point mutation lacking enzyme activity), into several hundred spatially grouped, glutamatergic or GABAergic neurons in rat POR cortex (the gene transfer conditions are detailed in the methods and in (Zhang et al., 2005)). Of note, we previously used phospho-specific antibodies in immunofluorescent costaining assays to show that PKC signaling pathways are activated in PkcΔ-transduced neurons (without visual learning), but not in control, PkcΔGG-transduced neurons (Zhang et al., 2005). In PkcΔ-transduced neurons, the phosphorylation levels of five PKC substrates were increased, specifically GAP-43, dynamin, AMPA receptor GluR2, NMDA receptor NR1, and MARCKS.

Here, we found that in the absence of visual learning, three learning-associated signaling pathways exhibit minimal activity in the transduced neurons. The rats were sacrificed at 10 days after gene transfer, without visual learning. The transduced neurons were visualized using an anti-flag antibody (PkcΔ and PkcΔGG contain the flag tag (Song et al., 1998)), and phosphorylation of CaMKII, MAP kinase, or CREB was visualized by costaining with anti-CaMKII-Thr286-P, anti-MAP Kinase-Thr202/Tyr204-P, or anti-CREB-Ser133-P, respectively. For rats that received either PkcΔ or PkcΔGG, we observed numerous transduced neurons (flag-immunoreactivity (IR) neurons), but these neurons contained only very low levels of costaining for phosphorylated CaMKII (PkcΔ, Figs. 1A–C; PkcΔGG, Figs. 2A–C), or phosphorylated MAP kinase (PkcΔ, Figs. 1D–F; PkcΔGG, Figs. 2D–F), or phosphorylated CREB (PkcΔ, Figs. 1G–I; PkcΔGG, Figs. 2G–I). The specificity of each of these commercially available phospho-specific antibodies has been established using Western blots. As a further control for the specificity of the assay, for a PkcΔ-transduced rat sacrificed after session 1 of learning (learning protocol below), omission of the primary antibodies resulted no detectable IR (Figs. 2J–L).

We quantified the levels of activation of each of these three signaling pathways in the transduced neurons by counting the transduced neurons that contained or lacked each phospho-protein. The results showed that for either the PkcΔ or PkcΔGG groups, <10% of the transduced neurons contained activated CaMKII or activated MAP kinase, and <15% of the transduced neurons contained activated CREB (Fig. 3; cell counts for each rat and each phospho-protein are in Supporting Information Tables S1–S3). Statistical comparisons showed that the PkcΔ- and PkcΔGG-transduced neurons contained statistically equivalent levels of costaining for each phospho-protein ($F_{(1,4)} = 0.086$; $F_{(1,4)} = 1.57$; $F_{(1,4)} = 0.119$, all $P > 0.05$). In summary, before visual learning, the PkcΔ-transduced neurons contain activated PKC pathways (Zhang et al., 2005), but these three learning-associated signaling pathways are predominately inactive.

During Learning of a New Visual Discrimination, PkcΔ-Transduced Neurons Exhibit Increased Learning-Associated Signaling Compared With Control PkcΔGG-Transduced Neurons

To perform visual learning, the rats press a lever to obtain an image set, cross the cage, and press their nose to a touchscreen to choose an image; correct choices are rewarded with food (Fig. 4A, schematic diagram of the apparatus; for additional details, see the Methods and Cook et al. (2004)). In our standard experimental design for visual learning (Fig. 4B) (Zhang et al., 2005, 2010a), rats learn a control image set before gene transfer (pre-gene-transfer image set, $\equiv$ vs. $||$), and after gene transfer of PkcΔ or controls (PkcΔGG or wt), rats are retested on this control image set, and then tested on an experimental, new image set (post-gene-transfer image set, []

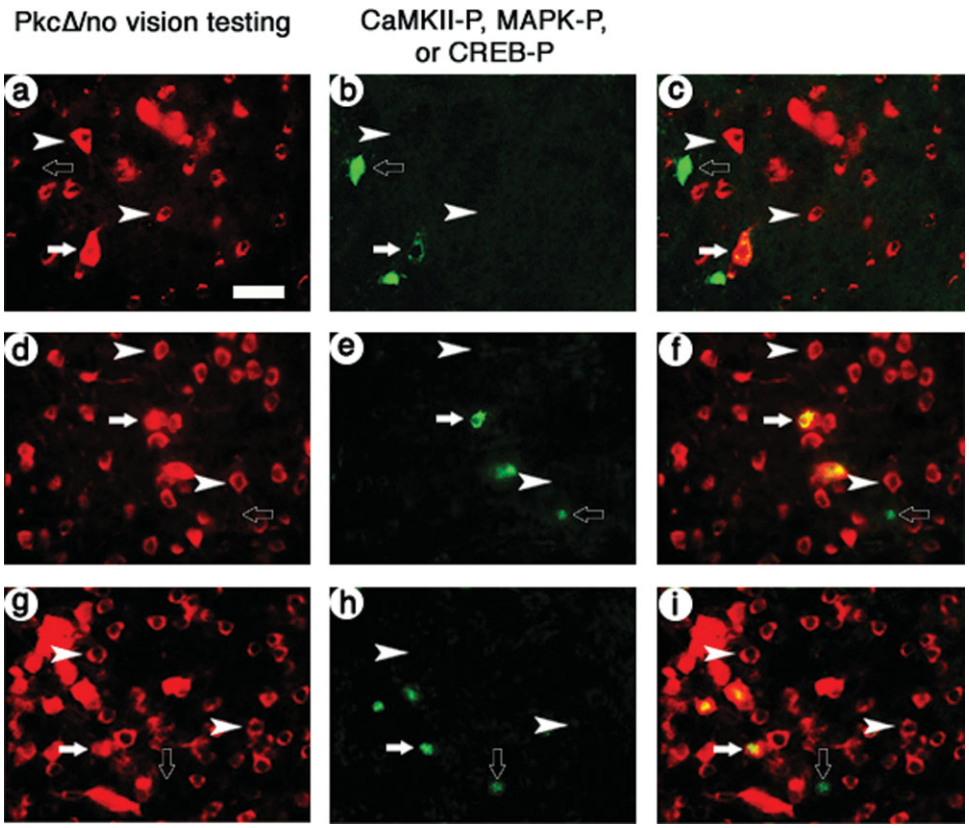

FIGURE 1. After gene transfer but before learning, the CaMKII, MAP kinase, and CREB pathways are inactive in PkcΔ-transduced neurons. (A–C) In a rat that received PkcΔ but no visual testing, the majority of the transduced cells lacked phosphorylated CaMKII; flag-IR (A), CaMKII-Thr286-P-IR (B), and merge (C). Arrows, costained cells; arrowheads, flag-IR only cells; empty arrows, phosphorylated protein-IR only cells. (D–F) Before visual testing, the vast majority of the PkcΔ-transduced cells lacked phosphorylated MAP kinase; flag-IR (D), MAP kinase-Thr202/Tyr204-P-IR (E), and merge (F). (G–I) Before visual testing, the majority of the PkcΔ-transduced cells lacked phosphorylated CREB; flag-IR (G), CREB-Ser133-P-IR (H), and merge (I). Scale bar: 50 μm. [Color figure can be viewed in the online issue, which is available at wileyonlinelibrary.com.]

vs. +). Previously, activity-dependent gene imaging (*c-fos, Arc, Zif268*) showed visual learning supports increased activity throughout POR cortex compared with a control of PkcΔ/no-visual-learning, which exhibited minimal activity (Zhang et al., 2005), as in other studies (Aggleton and Brown, 2005). Thus, our first hypothesis was that for control PkcΔGG rats during visual learning, the transduced neurons will exhibit increased learning-associated signaling compared with transduced neurons in the no-visual-learning condition. Further, activity-dependent gene imaging showed that during learning, the circuit containing PkcΔ-, but not PkcΔGG-, transduced neurons exhibited increased activity compared with the rest of POR cortex, but only during learning of a new, post-gene-transfer image set (Zhang et al., 2005, 2010a). This increased activity is tightly correlated with the enhanced learning, as each was observed only under the same conditions, PkcΔ rats tested on a new, post-gene-transfer image set (Zhang et al., 2005). Moreover, neurochemical lesions established that the genetically-modified circuit encodes some of the essential information for performance (Zhang et al., 2010a). [wt rats contain similar activated circuits during learning, but at different, unpredictable positions among the rats (Zhang et al., 2010a).] Thus, our second hypothesis was that for PkcΔ rats tested on a post-gene-transfer image set, the transduced neurons will exhibit increased learning-associated signaling compared with transduced neurons in the visual learning controls (PkcΔGG rats tested on a post-gene-transfer image set or PkcΔ rats retested on a pre-gene-transfer image set).

We examined the signaling in the identified, transduced neurons during visual learning, using our standard experimental design for the learning (Fig. 4B) (Zhang et al., 2005, 2010a) and the immunofluorescent costaining assays for phosphorylation of CaMKII, MAP kinase, or CREB. In a PkcΔ rat sacrificed after session 1 on the experimental, new, post-gene-transfer image set ([] vs. +), most transduced neurons also contained phosphorylated CaMKII (Figs. 5A–C); CaMKII is well known to be associated with glutamatergic synapses, and more recent studies found that CaMKII has important functions in GABAergic synapses (Marsden et al., 2010). In contrast, in a control condition, PkcΔGG rat sacrificed after session 1 on the post-gene-transfer image set, most transduced neurons lacked phosphorylated CaMKII (Figs. 5D–F). Similarly, in other PkcΔ rats sacrificed after session 1 on the post-gene-transfer image set, most transduced neurons contained phosphorylated MAP

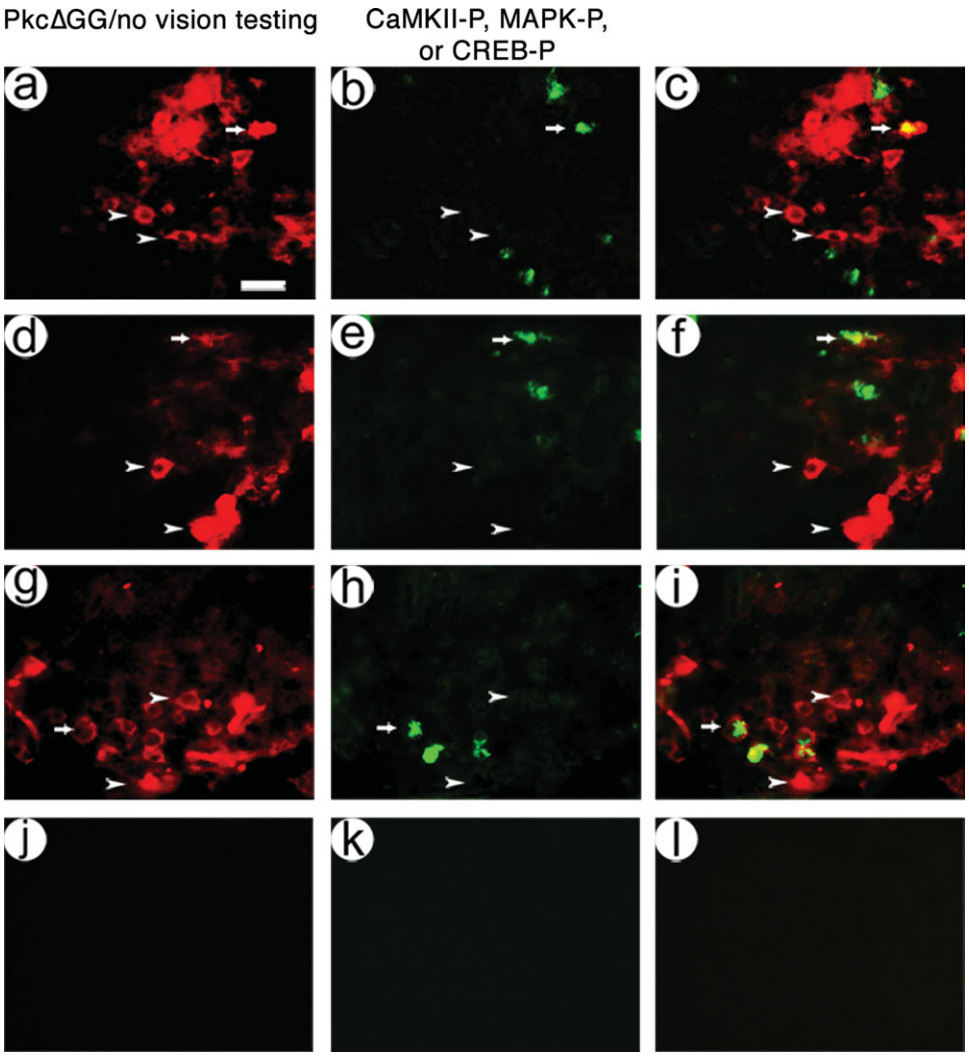

FIGURE 2. After gene transfer but before learning, the CaMKII, MAP kinase, and CREB pathways are inactive in PkcΔGG-transduced neurons. (A–C) Almost all PkcΔGG-transduced neurons lacked phosphorylated CaMKII; flag-IR (A), CaMKII-Thr286-P-IR (B), and merge (C). Arrows, costained cells; arrowheads, flag-IR only cells. (D–F) Almost all PkcΔGG-transduced neurons lacked phosphorylated MAP kinase; flag-IR (D), MAP kinase-Thr202/Tyr204-P-IR (E), and merge (F). (G–I) Almost all PkcΔGG-transduced neurons lacked phosphorylated CREB; flag-IR (G), CREB-Ser133-P-IR (H), and merge (I). (J–L) Omission of the primary antibodies resulted in no positive cells; fluorescein filter (J), rhodamine filter (K), and merge (L). Scale bar: 50 μm. [Color figure can be viewed in the online issue, which is available at wileyonlinelibrary.com.]

kinase (Figs. 6A–C) and phosphorylated CREB (Figs. 7A–C). In contrast, for control PkcΔGG rats sacrificed after session 1 on the post-gene-transfer image set, most transduced neurons lacked phosphorylated MAP kinase (Figs. 6D–F) and phosphorylated CREB (Figs. 7D–F). Further, for a PkcΔ rat retested on the control, pre-gene-transfer image set (‾ vs. |||, 10 sessions total), most transduced neurons lacked phosphorylated CREB (Figs. 7J–L). The control of PkcΔ/‾ vs. ||| supports similar accuracy before or after gene transfer ((Zhang et al., 2005) and below) and does not support increased activity in the genetically-modified circuit (Zhang et al., 2005); thus, we used the longest time point of 10 sessions as the most sensitive assay for any changes in CREB activity during retesting on the image set learned before gene transfer.

We quantified the levels of activation of each signaling pathway in the transduced neurons by cell counts (Fig. 3; data for each rat are in Supporting Information Tables S1–S3). For CaMKII, for the experimental condition, PkcΔ rats tested on the post-gene-transfer image set (PkcΔ/[] vs. +), 55 to 80% of the transduced neurons contained activated CaMKII; and over the 10 session testing period, the levels of activated CaMKII declined. In contrast, for a control condition, PkcΔGG/[] vs. +, only ~30% of the transduced neurons contained activated CaMKII. Statistical tests confirmed that the experimental group (PkcΔ/[] vs. +) contained the highest levels of activated CaMKII. A two-way ANOVA showed significant differences for group ($F_{(3,27)} = 82.4$, $P < 0.001$), and pair-wise comparisons (Student–Neumann–Keuls test) separately showed that the ex-

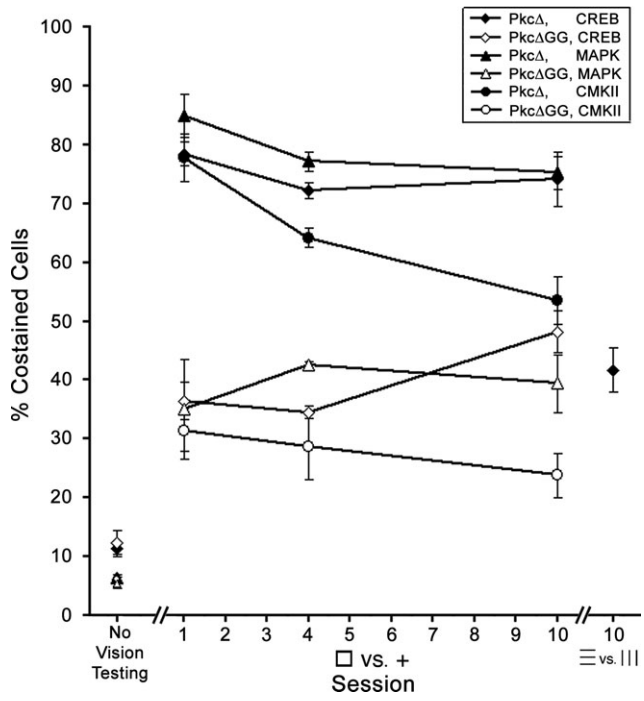

FIGURE 3. Cell counts of the levels of phosphorylated CaMKII, MAP kinase, and CREB in PkcΔ- or PkcΔGG-transduced neurons, either before or during the visual testing. For each condition, the % of the transduced neurons that contain a specific phospho-protein is shown (% costained cells, mean ± SEM). The visual testing experimental design is described in the text and diagrammed in Figure 4B.

perimental group contained higher levels of activated CaMKII than each control group (PkcΔ/[] vs. + compared with PkcΔGG/[] vs. +, PkcΔ/no-visual-testing, or PkcΔGG/no-visual-testing $P < 0.001$). Also, either vector with visual testing supported higher levels of activated CaMKII than either vector/no-visual-testing ($P < 0.001$).

Similar results were observed for both MAP kinase and CREB; the experimental condition of PkcΔ and the post-gene-transfer image set ([] vs. +) supported higher levels of phosphorylation than any of the controls. For MAP kinase, for the experimental condition, PkcΔ/[] vs. +, 75 to 85% of the transduced neurons contained activated MAP kinase; but for the control learning condition, PkcΔGG/[] vs. +, only 35 to 45% of the transduced neurons contained activated MAP kinase ($F_{(3,25)} = 120.0$, $P < 0.001$, two-way ANOVA. Pair-wise comparisons: PkcΔ/[] vs. + compared with PkcΔGG/[] vs. +, PkcΔ/no-visual-testing, or PkcΔGG/no-visual-testing, $P < 0.001$), and either vector with visual testing supported higher levels of activated MAP kinase than either vector/no-visual-testing ($P < 0.001$). Similarly, for CREB, for the experimental condition, PkcΔ/[] vs. +, 70 to 80% of the transduced neurons contained activated CREB; in contrast, for the two visual testing controls (PkcΔGG/[] vs. + or PkcΔ/— vs. | |) only 35 to 50% of the transduced neurons contained activated CREB ($F_{(4,32)} = 80.2$; $P < 0.001$ two-way ANOVA. Pair-wise comparisons: PkcΔ/[] vs. + compared with PkcΔGG/[] vs. +, PkcΔ/— vs. | |, or either vector/no-visual-testing, $P < 0.001$). Also, the two visual testing controls supported similar levels of activated CREB (PkcΔGG/[] vs. + compared with PkcΔ/— vs. | | $P > 0.05$), and either vector with visual testing supported higher levels of activated CREB than either vector/no-visual-testing ($P < 0.001$).

In PkcΔ-Transduced Neurons, Activated CaMKII Levels Declined During the Visual Testing Period, but Activated MAP Kinase and CREB Levels Remained Relatively Constant

First, we showed that PkcΔ supported higher levels of learning-associated signaling than PkcΔGG during both the initial learning and subsequent performance of the experimental, post-gene-transfer image set. Throughout testing on the post-gene-transfer image set, or for each of sessions 1, 4, or 10, PkcΔ supported higher levels of activation of each learning-associated signaling pathway than PkcΔGG (Fig. 3. Session 1, 4, or 10: CaMKII, $F_{(1,7)} = 80.4$, $F_{(1,4)} = 37.7$, $F_{(1,7)} = 25.7$; all $P < 0.005$; MAP kinase, $F_{(1,6)} = 40.1$, $F_{(1,4)} = 377.7$, $F_{(1,7)} = 48.4$, all $P < 0.001$; CREB, $F_{(1,6)} = 140.3$, $F_{(1,6)} = 351.7$, $F_{(2,12)} = 17.4$, all $P < 0.001$, one-way ANOVAs on each session and phospho-protein).

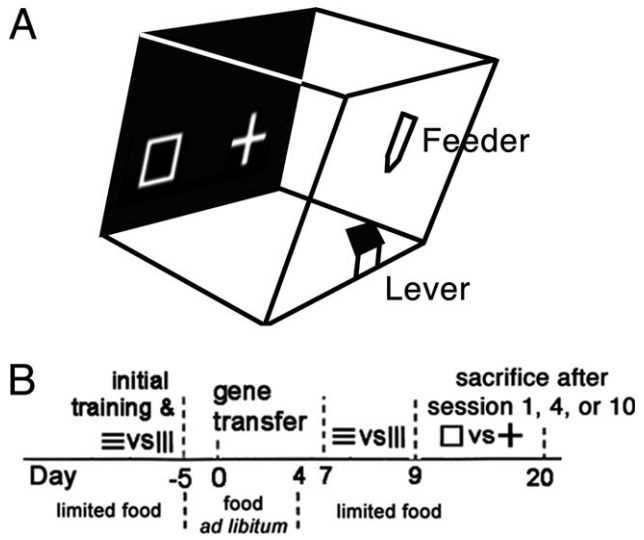

FIGURE 4. A schematic diagram of the visual testing apparatus, and a time line of the experimental design. (A) A schematic diagram of the testing apparatus. A rat starts a trial by pressing the lever, which causes two images to appear on the monitor. The rat then crosses the cage and presses a touchscreen to choose an image. Choosing the correct stimulus results in sound and food reward. After an incorrect response, a large solid rectangle is flashed on the monitor three times and the overhead houselight is turned off for 15 s. (B) A time line showing the experimental design. Rats were trained on the control, pre-gene-transfer image set (— vs. | |), gene transfer was performed (PkcΔ or control (PkcΔGG)); the rats were retested on the pre-gene-transfer image set, trained on the experimental, new, post-gene-transfer image set ([] vs. +) for 1, 4, or 10 sessions, and sacrificed. Additional details are in the Methods and in Cook et al. (2004).

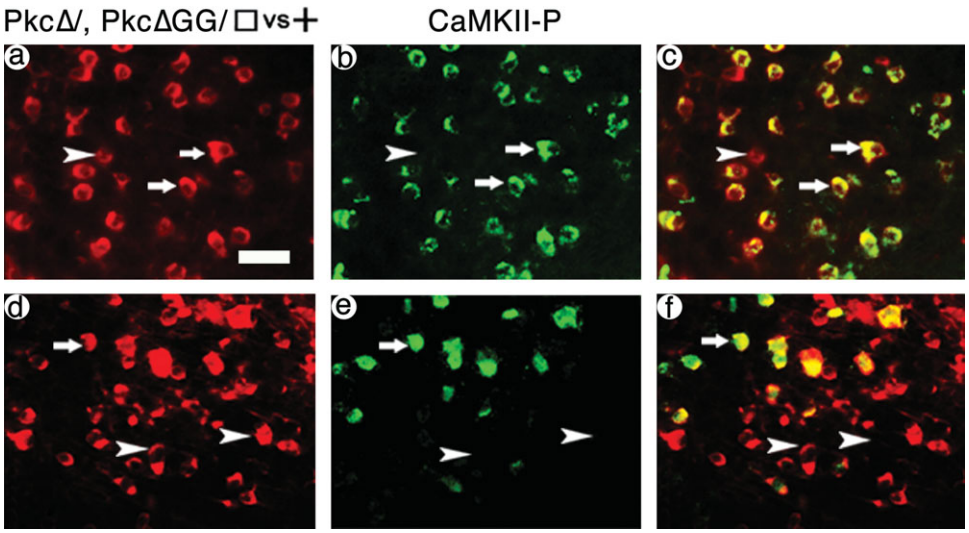

FIGURE 5. CaMKII is phosphorylated in PkcΔ-transduced neurons during visual learning. (A–C) After training for one session on the post-gene-transfer image set, most PkcΔ-transduced neurons contained phosphorylated CaMKII; flag-IR (A), CaMKII-Thr286-P-IR (B), and merge (C). Arrows, costained cells; arrowheads, flag-IR only cells. (D–F) After training for one session on the post-gene-transfer image set, most PkcΔGG-transduced neurons lacked phosphorylated CaMKII; flag-IR (D), CaMKII-Thr286-P-IR (E), and merge (F). Scale bar: 50 μm. [Color figure can be viewed in the online issue, which is available at wileyonlinelibrary.com.]

Next, we showed that PkcΔ supported higher levels of activated CaMKII during the initial learning than during subsequent performance; and, in contrast, the levels of activated MAP kinase and CREB were similar throughout testing. Of note, levels of activated CaMKII declined during testing on the post-gene-transfer image set: For PkcΔ, levels of activated CaMKII were higher during session 1 than sessions 4 or 10; and, as a control comparison, for PkcΔGG, levels of activated CaMKII were similar throughout visual testing (Fig. 3. Session: $F_{(3,27)} = 9.45$, $P < 0.001$; two-way ANOVA. PkcΔ: $F_{(2,10)} = 10.1$, $P < 0.005$, one-way ANOVA. Pair-wise comparisons: day 1 vs. day 4 $P = 0.059$, day 1 vs. day 10 $P < 0.005$, day 4 vs. day 10 $P = 0.10$. PkcΔGG: $F_{(2,9)} = 1.01$, $P > 0.05$). In contrast, for both PkcΔ and PkcΔGG, the levels of activated MAP kinase and CREB remained similar throughout testing on the post-gene-transfer image set (Fig. 3. Session: MAP ki-

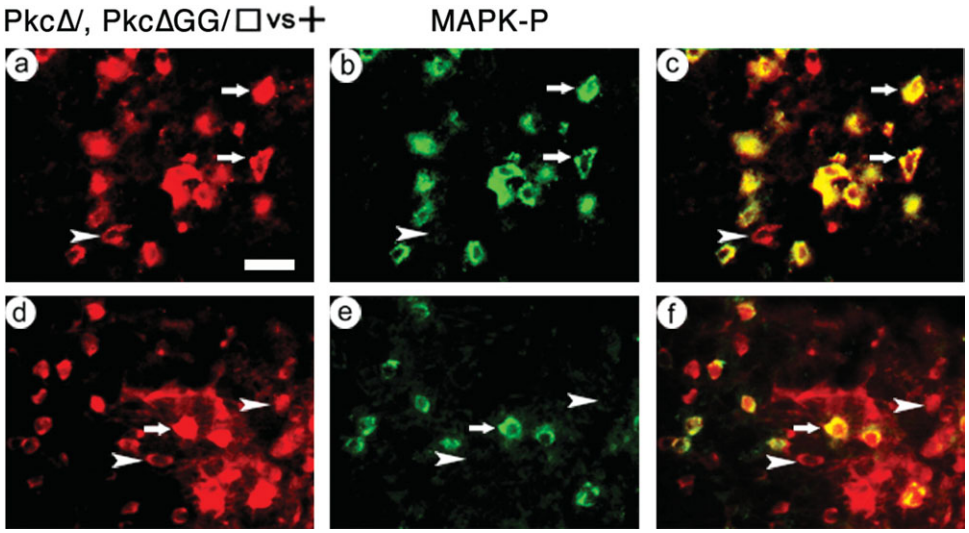

FIGURE 6. MAP kinase is phosphorylated in PkcΔ-transduced neurons during visual learning. (A–C) After training for one session on the post-gene-transfer image set ([] vs. +), most PkcΔ-transduced neurons contained phosphorylated MAP kinase; flag-IR (A), MAP kinase-Thr202/Tyr204-P-IR (B), and merge (C). Arrows, costained cells; arrowheads, flag-IR only cells. (D–F) After training for one session on the post-gene-transfer image set, most PkcΔGG-transduced neurons lacked phosphorylated MAP kinase; flag-IR (D), MAP kinase-Thr202/Tyr204-P-IR (E), and merge (F). Scale bar: 50 μm. [Color figure can be viewed in the online issue, which is available at wileyonlinelibrary.com.]

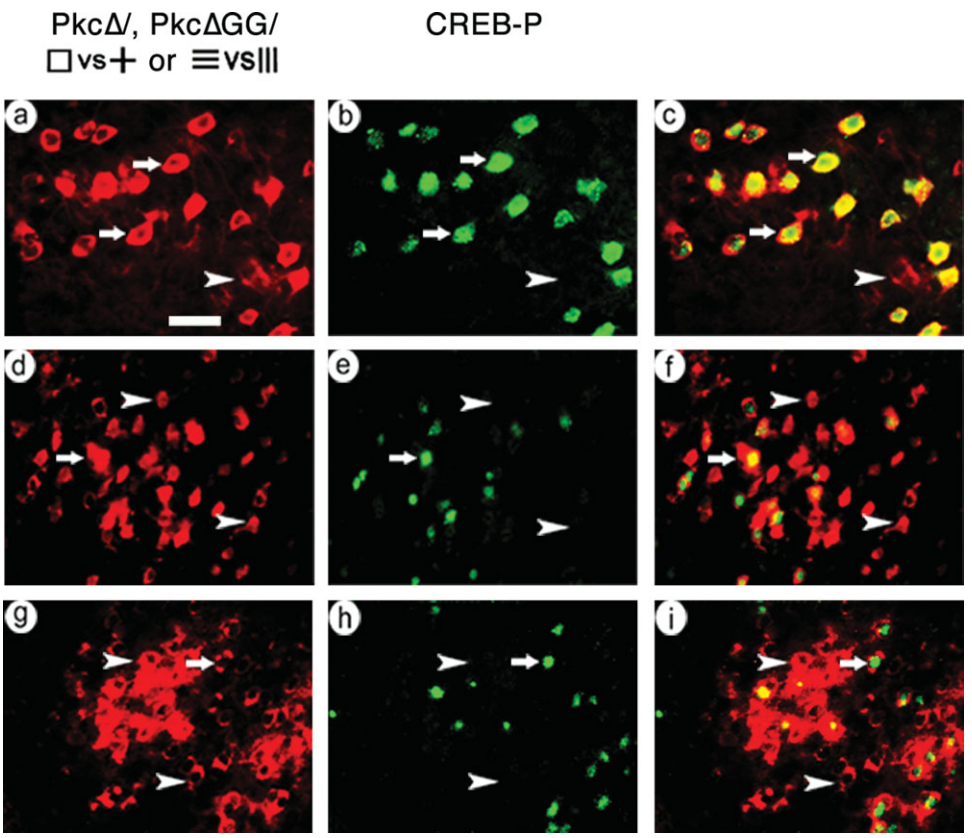

FIGURE 7. CREB is phosphorylated in PkcΔ-transduced neurons during learning of a post-gene-transfer image set. (A–C) After training for one session on the post-gene-transfer image set ([] vs. +), most PkcΔ-transduced neurons contained phosphorylated CREB; flag-IR (A), CREB-Ser133-P-IR (B), and merge (C). Arrows, costained cells; arrowheads, flag-IR only cells. (D–F) After training for one session on the post-gene-transfer image set, most PkcΔGG-transduced neurons lacked phosphorylated CREB; flag-IR (D), CREB-Ser133-P-IR (E), and merge (F). (G–I) For a rat that received PkcΔ and retesting on the pre-gene-transfer image set (— vs. ||) most transduced neurons lacked phosphorylated CREB; flag-IR (G), CREB-Ser133-P-IR (H), and merge (I). Scale bar: 50 μm. [Color figure can be viewed in the online issue, which is available at wileyonlinelibrary.com.]

nase, $F_{(2,26)} = 0.79$ $P > 0.05$; CREB, $F_{(2,34)} = 2.96$, $P > 0.05$, two-way ANOVAs on each phospho-protein).

In PkcΔ-Transduced Neurons, During Visual Learning, MAP Kinase and CREB Were Phosphorylated to Similar Levels, Which Were Higher Than Those for CaMKII

If a specific signaling pathway activates a particular signaling pathway, then these two pathways should display activation in a similar fraction of the transduced neurons; of note, the MAP kinase pathway can activate the CREB pathway. Thus, we compared the levels of activation of the three pathways during the visual learning. We found that during the initial learning (session 1), the three pathways were activated to similar levels; but with additional training (session 4), or during performance (session 10), MAP kinase and CREB were activated at similar levels, which were higher than those for CaMKII (Fig. 3. Phospho-protein: $F_{(2,37)} = 10.0$, $P < 0.001$, two-way ANOVA. Pair-wise comparisons: MAP kinase or CREB vs. CaMKII $P < 0.01$, MAP kinase vs. CREB $P > 0.05$. Session: $F_{(2,37)} = 10.4$, $P < 0.001$; session 1 vs. session 4 or 10 $P < 0.02$, session 4 vs. session 10 $P > 0.05$. Session 1: $F_{(2,11)} = 1.48$, $P > 0.05$, one-way ANOVA. Session 4: $F_{(2,5)} = 18.2$, $P < 0.006$; MAP kinase or CREB vs. CaMKII $P < 0.025$, MAP kinase vs. CREB $P > 0.05$. Session 10: $F_{(2,15)} = 9.99$, $P < 0.003$; MAP kinase or CREB vs. CaMKII $P < 0.005$, MAP kinase vs. CREB $P > 0.05$).

For a control comparison, we compared activation of these three pathways in the PkcΔGG-transduced neurons during learning of the post-gene-transfer image set. MAP kinase and CREB were activated to similar levels, and higher than those for CaMKII, but there were no significant changes during the testing period (Fig. 3. Phospho-protein: $F_{(2,32)} = 8.58$, $P < 0.002$, two-way ANOVA. Session: $F_{(2,32)} = 4.10$, $P > 0.05$).

PkcΔ Supports Higher Accuracy Than Control Conditions on the Experimental Image Sets Learned After Gene Transfer

In our standard experimental design for visual learning (Fig. 4B), the rats learn a control image set before gene transfer (pre-gene-transfer image set, — vs. ||); and after gene transfer, the rats are retested on this control image set, and then they learn

an experimental, new image set (post-gene-transfer image set, [] vs. +). We previously showed that before gene transfer, the groups exhibited similar accuracy for learning the control, pre-gene-transfer image set (= vs. ||), and, after gene transfer, the PkcΔ or control groups (PkcΔGG, ß-gal, PBS, or wt (no surgery)) exhibited statistically similar accuracy for retesting on this control image set (Zhang et al., 2005). In contrast, and most importantly, the PkcΔ groups showed statistically significant higher accuracy than the controls on two experimental, new, post-gene-transfer image sets (the image set used here, [] vs. +; and / vs. \) (Zhang et al., 2005). In the present experiment on learning-associated signaling pathways, after gene transfer, the PkcΔ and control PkcΔGG groups showed similar accuracy on retesting for the control, pre-gene-transfer image set (Fig. 8A left, = vs. || $F_{(1,22)} = 3.12$, $P > 0.05$). In contrast, for the experimental, post-gene-transfer image set, the PkcΔ group showed a difference in accuracy that approached statistical significance compared with the control PkcΔGG group (Fig. 8A right, [] vs. + $F_{(1,114)} = 3.40$, $P = 0.068$). The pattern of the results for these conditions replicates our earlier findings. The marginally significant effect of group observed here appears to be due to the smaller group sizes ($n = 6$ rats/group) required for the present assays, whereas our earlier demonstrations of enhanced learning typically used group sizes of ~9 to 12 rats (Zhang et al., 2005).

To confirm that PkcΔ supports higher accuracy than controls, we performed additional experiments with group sizes (8–17 rats) similar to our initial demonstrations of enhanced learning (Zhang et al., 2005); because enhanced learning typically produces smaller effects than deficits in learning (see discussion), we performed three independent experiments. In these experiments, before gene transfer, the rats learned the control pre-gene transfer image set (= vs. ||); after gene transfer, the rats were retested on this control, pre-gene-transfer image set, and then tested sequentially on two experimental, post-gene-transfer image sets (/ vs. \ then [] vs. +). The results showed that after gene transfer, the groups exhibited statistically similar accuracy for retesting on the control, pre-gene-transfer image set, in each of the three experiments (Fig. 8B left, = vs. || $F_{(1,28)} = 0.501$, $P > 0.05$, PkcΔ $n = 6$ rats, wt (no surgery) $n = 10$ rats. Fig. 8C left, = vs. || $F_{(1,58)} = 1.410$, $P > 0.05$, PkcΔ $n = 13$ rats, wt $n = 17$ rats. Fig. 8D left, = vs. || $F_{(1,38)} = 1.064$, $P > 0.05$, PkcΔ $n = 8$ rats, PkcΔGG $n = 12$ rats). In contrast, the results showed that the PkcΔ groups exhibited statistically significant higher accuracy than the controls, for both experimental, post-gene-transfer image sets, in each of the three independent experiments (Fig. 8B middle, / vs. \ $F_{(1,80)} = 5.24$, $P < 0.03$, PkcΔ $n = 8$ rats, wt $n = 9$ rats. Fig. 8B right, [] vs. + $F_{(1,83)} = 4.65$, $P < 0.035$, PkcΔ $n = 8$ rats, wt $n = 10$ rats. Fig. 8C middle, / vs. \ $F_{(1,145)} = 4.67$, $P < 0.035$, PkcΔ $n = 13$ rats, wt $n = 17$ rats. Fig. 8C right, [] vs. + $F_{(1,147)} = 10.4$, $P < 0.005$, PkcΔ $n = 13$ rats, wt $n = 16$ rats. Fig. 8D middle, / vs. \ $F_{(1,95)} = 8.17$, $P < 0.01$, PkcΔ $n = 8$ rats, PkcΔGG $n = 12$ rats. Fig. 8D right, [] vs. + $F_{(1,98)} = 7.17$, $P < 0.03$, PkcΔ $n = 8$ rats, PkcΔGG $n = 12$ rats). In some experiments, procedural errors resulted in modest differences in group size on different image sets. All the statistical tests for post-gene-transfer image sets examined sessions 6 to 10, as previously examined (Zhang et al., 2005); nonetheless, statistical tests for sessions 1 to 10 showed the same significant differences. In summary, PkcΔ and controls supported similar accuracy for retesting on the control, pre-gene-transfer image set, in eight independent experiments (five in (Zhang et al., 2005), three here). In contrast, PkcΔ increased accuracy compared with controls for testing on two experimental, post-gene-transfer image sets, in seven independent experiments on [] vs. + (four in (Zhang et al., 2005), three here), and in four independent experiments on / vs. \ (one in (Zhang et al., 2005), three here).

Combining the data from these three experiments yielded the same pattern of results. For retesting on the control, pre-gene-transfer image set (= vs. ||) the three groups (PkcΔ, PkcΔGG, and wt) were statistically similar ($F_{(2,127)} = 1.50$, $P > 0.05$). In contrast, PkcΔ increased accuracy compared with each control for testing on each of the two experimental, post-gene-transfer image sets, and the controls were similar (/ vs. \ $F_{(2,323)} = 9.28$, $P < 0.001$; PkcΔ vs. PkcΔGG or wt $P < 0.001$; PkcΔGG vs. wt $P > 0.05$. [] vs. + $F_{(2,331)} = 10.8$, $P < 0.001$; PkcΔ vs. PkcΔGG or wt $P < 0.001$; PkcΔGG vs. wt $P > 0.05$).

The two post-gene-transfer image sets, / vs. \ and [] vs. +, are of moderate difficulty, and most rats learned these image sets in 4 to 6 sessions (Fig. 8 and Zhang et al. 2005). In the three present experiments, the PkcΔ rats learned / vs. \ to a higher accuracy than [] vs. +; in two of these experiments, the control rats learned / vs. \ to a higher accuracy than [] vs. +; and in the third experiment, the control rats learned the two image sets to similar accuracies (/ vs. \ compared with [] vs. +: Fig. 8B, PkcΔ $F_{(1,77)} = 10.6$, $P < 0.005$, wt $F_{(1,86)} = 2.40$, $P > 0.05$; Fig. 8C, PkcΔ $F_{(1,122)} = 4.09$, $P < 0.05$, wt $F_{(1,160)} = 7.14$, $P < 0.01$; Fig. 8D, PkcΔ $F_{(1,76)} = 11.1$, $P < 0.002$, PkcΔGG $F_{(1,117)} = 4.95$, $P < 0.03$).

DISCUSSION

Here, we establish that during the learning and performance of visual shape discriminations, three learning-associated signaling pathways are coactivated in identified neurons that are part of a neocortical circuit that encodes some of the essential information for performance (Zhang et al., 2010a). We previously showed that visual learning supports increased neuronal activity throughout POR cortex (Zhang et al., 2005, 2010a). Consistent with this observation, and supporting our first hypothesis, after gene transfer but before learning, the three learning-associated signaling pathways were predominately inactive, and visual learning increased activity in these three learning-associated signaling pathways, in the transduced neurons. Of note, we previously showed the genetically-modified circuit encodes essential information for performance, and exhibits increased activity during performance (Zhang et al., 2005, 2010a). Consistent

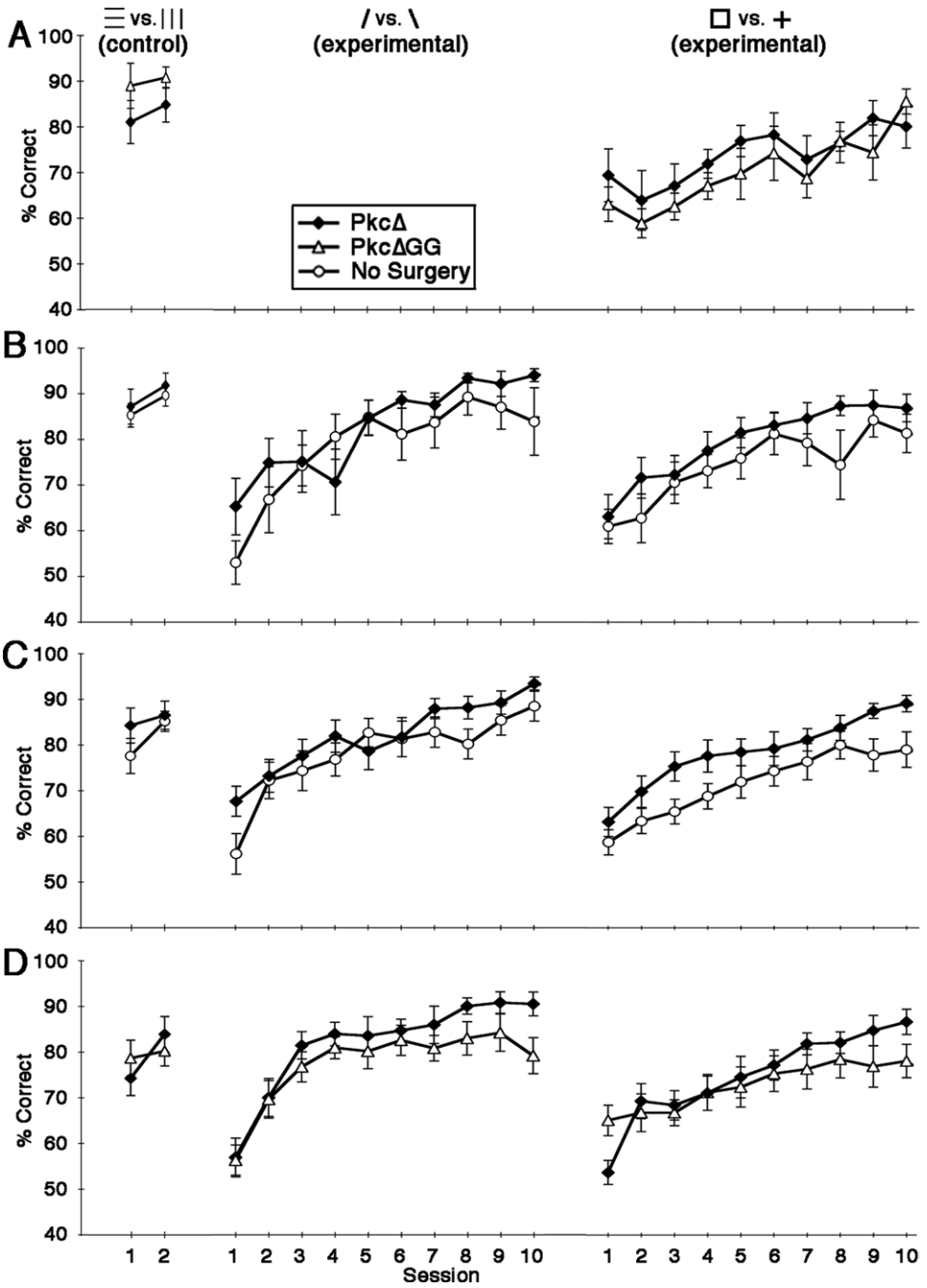

FIGURE 8. Delivery of PkcΔ into neurons in POR cortex enhances accuracy on two experimental, new, post-gene-transfer image sets. Rats were trained on the control, pre-gene-transfer image set (☰ vs. |||); gene transfer was performed; and the rats were retested on this control, pre-gene-transfer image set, and then trained on experimental, new, post-gene-transfer image sets (/ vs. \, [] vs. +). Additional details are in the methods. (A) The rats used in the phosphorylation experiments. (B–D) Rats from three additional independent experiments.

with these observations, and supporting our second hypothesis, during the learning of new image sets, the transduced neurons contained elevated activity in these three learning-associated signaling pathways, compared with transduced neurons in the visual learning control conditions. Interestingly, during early learning, these three pathways were activated to similar levels, but as learning reached steady-state levels later in the testing, CaMKII activity declined, whereas MAP kinase and CREB activity remained high.

An important advantage of the enhanced learning approach used here is that selective modification of a specific circuit enables the function of that circuit to be examined, as in this study, but the magnitude of the enhanced learning appears to be modest (as previously discussed (Zhang et al., 2005)). The

magnitude of enhanced learning usually reported in the literature, and observed here, is usually more modest than the magnitude of decreased learning typically observed using knockouts or lesions. For instance, transgenic mice that overexpress the NMDA receptor NR2B subunit displayed modest increases in performance using several tests of learning (Tang et al., 1999). Further, pharmacological interventions that enhance learning also typically produce modest increases in performance; for example, following systemic administration of specific opiate agonists, modest enhancements in working memory are observed in the radial arm maze (Canli et al., 1990). Similar to our results, overexpression of another constitutively active PKC, PKMζ, in insular cortex caused a significant increase in the rate of conditioned taste aversion learning, but only a modest enhancement in steady state performance (Shema et al., 2011). The maximum possible level of performance is one reason for this difference. This is because significant improvements in learning capability can support only modest increases in accuracy or other measures of performance, as the system is probably operating relatively efficiently (Rumelhart et al., 1986; Dudai, 1989). Animals are likely close to their maximum potential performance level during learning; thus, it is easier to increase performance early in training (for example, from 55 to 65%) than after a task is largely acquired (for example, from 80 to 90%). Moreover, learning processes likely map nonlinearly onto accuracy and other dependent variables. Thus, there is usually more space to observe decreased, than increased, performance. For example, as our rats achieved ~80% correct, a lesion that reduced learning to chance would cause an ~30% decrease in accuracy, whereas a 30% increase would be impossible to measure. Given these considerations, it is possible that modest increases in observed performance may reflect substantial increases in information processing efficacy. Consistent with these observations, and indicating the critical role of PKC pathways in learning, large deficits were observed after inhibiting a specific PKC isoform in a specific brain area, or lesioning a critical circuit after PKC-dependent learning: Blocking PKMζ activity throughout insular cortex by infusing a small drug, or blocking PKMζ activity in many insular cortex neurons by expressing a dominant negative PKMζ, caused large deficits in conditioned taste aversion learning (Shema et al., 2007, 2011). Also, after gene transfer of PkcΔ and learning new image sets, NMDA-mediated lesioning of the genetically-modified circuit in POR cortex caused large deficits in performance (Zhang et al., 2010a).

During visual learning, the three learning-associated signaling pathways were activated in the transduced neurons, and this activation could be supported by specific combinations of increased protein phosphorylation and increased protein levels. We did not attempt to quantify protein levels in the transduced neurons because no straightforward method is available; we did not perform Western blots because the transduced neurons would represent only a small fraction of the cells in tissue punches containing the injection site. Nonetheless, after gene transfer of either vector, but before learning, the percentages of transduced neurons that contained each phospho-protein were low (<10% for CaMKII and MAP kinase, and <15% for CREB), and there were large increases in the percentages of PkcΔ-transduced neurons that contained each phospho-protein, to 78 to 85%, after the first session on the new image set. These increases in phospho-protein levels were rapid, since a session lasts at most 1 h, and the rats were sacrificed within 30 min after the session. Synthesis of new CaMKII protein can be rapid, occurring in less than 5 min. However, it seems unlikely that in less than 90 min, new synthesis of all three of these proteins accounted for the majority of the changes in phosphorylation levels.

During learning, these three signaling proteins were likely cophosphorylated in the same PkcΔ-transduced neurons. We did not perform triple staining assays to simultaneously examine two learning-associated signaling pathways in the same transduced neurons. But even if each protein were phosphorylated independent of the other two, then after session 1, 52% of the PkcΔ-transduced neurons would contain all three phospho-proteins (78, 85, or 78% of the flag-IR cells costained for CaMKII-P, MAP kinase-P, or CREB-P, respectively; $0.78 \times 0.85 \times 0.78 = 0.52$), and at least 61% of the PkcΔ-transduced neurons would contain any combination of two of these phospho-proteins; and after sessions 4 or 10, at least 56% of the PkcΔ-transduced neurons would contain both phosphorylated MAP kinase and phosphorylated CREB.

Several types of evidence suggest a causal relationship between the phosphorylation of MAP kinase and CREB in PKcΔ-transduced neurons during learning of a new image set. First, the percentage of PkcΔ-transduced neurons that contained phosphorylated MAP kinase and CREB were similar at session 1, 4, and 10, ~80%. Second, as noted above, the changes in the levels of these phospho-proteins occurred simultaneously and rapidly with learning a new image set. Third, activated MAP kinase can phosphorylate CREB, although CREB can also be phosphorylated by other kinases, notably the cAMP-dependent protein kinase (PKA). Thus, the results suggest that activated MAP kinase phosphorylated CREB.

Activation of these three learning-associated signaling pathways may play an important role in visual learning as activation occurred preferentially in the specific conditions associated with this learning, specifically, activation required both the constitutively active PKC and learning a new image set. After gene transfer of the constitutively active PKC, but before learning, five PKC pathways were activated, but these three learning-associated signaling pathways remained inactive; specifically, we observed increased phosphorylation of the PKC substrates GAP-43, dynamin, AMPA receptor GluR2, NMDA receptor NR1, and MARCKS (Zhang et al., 2005); but CaMKII, MAP kinase, and CREB were not phosphorylated above control levels. Importantly, after gene transfer of the constitutively active PKC, and upon learning a new image set, these three learning-associated signaling pathways were activated to high levels, and to higher levels than in the two control learning conditions (the constitutively active PKC, but retesting on a control image set learned before gene transfer; or the control PKC that lacks

activity, and learning a new image set). In summary, the experimental condition, the constitutively active PKC and learning a new image set, activated these three learning-associated signaling pathways, increased neuronal activity in the genetically-modified circuit, enhanced accuracy for the visual discriminations, and encoded some of the essential information for performance in the genetically-modified circuit; further, these changes were not observed under the two control learning conditions (Zhang et al., 2005, 2010a). Together, these results strongly suggest that these three learning-associated signaling pathways play an important role in the learning.

Although it is well established that each of these three learning-associated signaling pathways is required for specific cognitive learning tasks (Silva et al., 1992, 1998; Bozon et al., 2003; Elgersma et al., 2004; Sweatt, 2004; Wayman et al., 2008), there is limited information about the specific circuits and neurons that require each pathway, and at which specific times, for performing a specific learning task. The CaMKII and CREB pathways are required for multiple learning tasks, as shown using knockout mice (Silva et al., 1992, 1998; Elgersma et al., 2004). Further, deficits in hippocampal long-term potentiation, spatial learning, and other hippocampal-dependent tasks suggest that hippocampal circuits are required. Moreover, a requirement for CREB in hippocampal circuits for spatial learning was directly shown by local infusion of an antisense oligonucleotide (Guzowski and McGaugh, 1997). Analogously, CREB activity in perirhinal cortex circuits is required for long-term recognition memory; delivery of a dominant negative CREB into some perirhinal cortex neurons blocks this learning (Warburton et al., 2005). Correlatively, CREB is required in neurons in specific subcortical areas for specific simple learning tasks, including in the basal lateral amygdala neurons for fear conditioning (Han et al., 2007), and in mitral cells of the olfactory bulb for early odor preference learning (Yuan et al., 2003). Similarly, MAP kinase is required in specific forebrain areas for specific cognitive tasks, as shown by local infusion of drugs (Sweatt, 2001); for example, MAP kinase activity in entorhinal cortex is required for spatial learning (Hebert and Dash, 2002) and MAP kinase activity in the dentate gyrus and entorhinal cortex are required for recognition learning (Kelly et al., 2003). The level of specificity in these studies is at best that one specific signaling pathway is required in a specific forebrain area for a specific type of cognitive task, and many studies contain less resolution. Our results advance this important literature by showing that three learning-associated signaling pathways are activated, at specific times during learning, in identified neurons in an essential circuit within a specific neocortical area (Zhang et al., 2010a).

The present results are consistent with synaptic plasticity and neural network theories that hypothesize that the activity of specific signaling pathways, in specific neurons, modify synaptic strengths, thereby encoding essential information for performance (Rumelhart et al., 1986; Dudai, 1989). While specific signaling pathways are known to be required for learning (Silva et al., 1992, 1998; Bozon et al., 2003; Elgersma et al., 2004; Sweatt, 2004; Wayman et al., 2008), this is the first demonstration that three specific signaling pathways are activated during learning in identified neurons that are part of a neocortical circuit that encodes some essential information for cognitive learning.

Acknowledgments

The authors gratefully thank Dr. A. Davison for HSV-1 cosmid set C, Dr. K. O'Malley for the TH promoter, Dr. G. Felsenfeld for ß-globin insulator, and Dr. W. Schlaepfer for the NFH promoter. The authors also thank J. Dougherty for technical assistance. A.I.G. has equity in Alkermes, Inc.

REFERENCES

Abeliovich A, Paylor R, Chen C, Kim JJ, Wehner JM, Tonegawa S. 1993. PKC gamma mutant mice exhibit mild deficits in spatial and contextual learning. Cell 75:1263–1271.

Aggleton JP, Brown MW. 2005. Contrasting hippocampal and perirhinal cortex function using immediate early gene imaging. Q J Exp Psychol B 58:218–233.

Bozon B, Kelly A, Josselyn SA, Silva AJ, Davis S, Laroche S. 2003. MAPK, CREB and zif268 are all required for the consolidation of recognition memory. Philos Trans R Soc Lond B Biol Sci 358:805–814.

Burwell RD, Amaral DG. 1998. Perirhinal and postrhinal cortices of the rat: interconnectivity and connections with the entorhinal cortex. J Comp Neurol 391:293–321.

Canli T, Cook RG, Miczek KA. 1990. Opiate antagonists enhance the working memory of rats in the radial maze. Pharmacol Biochem Behav 36:521–525.

Cook RG, Geller AI, Zhang G, Gowda R. 2004. Touchscreen enhanced visual learning in rats. Behav Res Methods Instrum Comput 36:101–106.

Dudai Y. 1989. The Neurobiology of Memory. Oxford, England: Oxford University Press.

Dudai Y. 2004. The neurobiology of consolidations, or, how stable is the engram? Annu Rev Psychol 55:51–86.

Elgersma Y, Sweatt JD, Giese KP. 2004. Mouse genetic approaches to investigating calcium/calmodulin-dependent protein kinase II function in plasticity and cognition. J Neurosci 24:8410–8415.

Fraefel C, Song S, Lim F, Lang P, Yu L, Wang Y, Wild P, Geller AI. 1996. Helper virus-free transfer of herpes simplex virus type 1 plasmid vectors into neural cells. J Virol 70:7190–7197.

Frankland PW, Bontempi B. 2005. The organization of recent and remote memories. Nat Rev Neurosci 6:119–130.

Guzowski JF, McGaugh JL. 1997. Antisense oligodeoxynucleotide-mediated disruption of hippocampal cAMP response element binding protein levels impairs consolidation of memory for water maze training. Proc Natl Acad Sci USA 94:2693–2698.

Han JH, Kushner SA, Yiu AP, Cole CJ, Matynia A, Brown RA, Neve RL, Guzowski JF, Silva AJ, Josselyn SA. 2007. Neuronal competition and selection during memory formation. Science 316:457–460.

Hanks SK, Quinn AM, Hunter T. 1988. The protein kinase family: Conserved features and deduced phylogeny of the catalytic domains. Science 241:42–52.

Hebert AE, Dash PK. 2002. Extracellular signal-regulated kinase activity in the entorhinal cortex is necessary for long-term spatial memory. Learn Mem 9:156–166.

Kelly A, Laroche S, Davis S. 2003. Activation of mitogen-activated protein kinase/extracellular signal-regulated kinase in hippocampal

circuitry is required for consolidation and reconsolidation of recognition memory. J Neurosci 23:5354–5360.

Lim F, Hartley D, Starr P, Lang P, Song S, Yu L, Wang Y, Geller AI. 1996. Generation of high-titer defective HSV-1 vectors using an IE 2 deletion mutant and quantitative study of expression in cultured cortical cells. Biotechniques 20:460–469.

Ling DS, Benardo LS, Serrano PA, Blace N, Kelly MT, Crary JF, Sacktor TC. 2002. Protein kinase Mzeta is necessary and sufficient for LTP maintenance. Nat Neurosci 5:295–296.

Marsden KC, Shemesh A, Bayer KU, Carroll RC. 2010. Selective translocation of Ca2+/calmodulin protein kinase IIalpha (CaMKIIalpha) to inhibitory synapses. Proc Natl Acad Sci USA 107:20559–20564.

McClelland JL, McNaughton BL, O'Reilly RC. 1995. Why there are complementary learning systems in the hippocampus and neocortex: Insights from the successes and failures of connectionist models of learning and memory. Psychol Rev 102:419–457.

Moser MB, Moser EI. 1998. Distributed encoding and retrieval of spatial memory in the hippocampus. J Neurosci 18:7535–7542.

Murray EA, Bussey TJ, Saksida LM. 2007. Visual perception and memory: A new view of medial temporal lobe function in primates and rodents. Annu Rev Neurosci 30:99–122.

Nadel L, Moscovitch M. 1997. Memory consolidation, retrograde amnesia and the hippocampal complex. Curr Opin Neurobiol 7:217–227.

Neill JC, Sarkisian MR, Wang Y, Liu Z, Yu L, Tandon P, Zhang G, Holmes GL, Geller AI. 2001. Enhanced auditory reversal learning by genetic activation of protein kinase C in small groups of rat hippocampal neurons. Mol Brain Res 93:127–136.

Oh JD, Geller AI, Zhang G, Chase TN. 2003. Gene transfer of constitutively active protein kinase C into striatal neurons accelerates onset of levodopa-induced motor response alterations in parkinsonian rats. Brain Res 971:18–30.

Pastalkova E, Serrano P, Pinkhasova D, Wallace E, Fenton AA, Sacktor TC. 2006. Storage of spatial information by the maintenance mechanism of LTP. Science 313:1141–1144.

Paxinos G, Watson C. 1986. The Rat Brain in Stereotaxic Coordinates. Sidney: Academic Press.

Rumelhart DE, McClelland JL, Group PR. 1986. Parallel Distributed Processing. Cambridge, MA: MIT Press.

Shema R, Haramati S, Ron S, Hazvi S, Chen A, Sacktor TC, Dudai Y. 2011. Enhancement of consolidated long-term memory by overexpression of protein kinase Mzeta in the neocortex. Science 331:1207–1210.

Shema R, Sacktor TC, Dudai Y. 2007. Rapid erasure of long-term memory associations in the cortex by an inhibitor of PKM zeta. Science 317:951–953.

Silva AJ, Kogan JH, Frankland PW, Kida S. 1998. CREB and memory. Annu Rev Neurosci 21:127–148.

Silva AJ, Paylor R, Wehner JM, Tonegawa S. 1992. Impaired spatial learning in alpha-calcium-calmodulin kinase II mutant mice. Science 257:206–211.

Song S, Wang Y, Bak SY, During MJ, Bryan J, Ashe O, Ullrey DB, Trask LE, Grant FD, O'Malley KL, Riedel H, Goldstein DS, Neve KA, LaHoste GJ, Marshall JF, Haycock JW, Neve RL, Geller AI. 1998. Modulation of rat rotational behavior by direct gene transfer of constitutively active protein kinase C into nigrostriatal neurons. J Neurosci 18:4119–4132.

Squire LR, Alvarez P. 1995. Retrograde amnesia and memory consolidation: A neurobiological perspective. Curr Opin Neurobiol 5:169–177.

Sun M, Kong L, Wang X, Holmes C, Gao Q, Zhang W, Pfeilschifter J, Goldstein DS, Geller AI. 2004. Coexpression of tyrosine hydroxylase, GTP cyclohydrolase I, aromatic amino acid decarboxylase, and vesicular monoamine transporter-2 from a helper virus-free HSV-1 vector supports high-level, long-term biochemical and behavioral correction of a rat model of Parkinson's disease. Hum. Gene Ther 15:1177–1196.

Sun M, Zhang GR, Yang T, Yu L, Geller AI. 1999. Improved titers for helper virus-free herpes simplex virus type 1 plasmid vectors by optimization of the packaging protocol and addition of noninfectious herpes simplex virus-related particles (previral DNA replication enveloped particles) to the packaging procedure. Hum Gene Ther 10:2005–2011.

Sweatt JD. 2001. The neuronal MAP kinase cascade: A biochemical signal integration system subserving synaptic plasticity and memory. J Neurochem 76:1–10.

Sweatt JD. 2004. Mitogen-activated protein kinases in synaptic plasticity and memory. Curr Opin Neurobiol 14:311–317.

Tanaka C, Nishizuka Y. 1994. The protein kinase C family for neuronal signaling. Ann Rev Neurosci 17:551–567.

Tang YP, Shimizu E, Dube GR, Rampon C, Kerchner GA, Zhuo M, Liu G, Tsien JZ. 1999. Genetic enhancement of learning and memory in mice. Nature 401:63–69.

Van der Gucht E, Clerens S, Cromphout K, Vandesande F, Arckens L. 2002. Differential expression of c-fos in subtypes of GABAergic cells following sensory stimulation in the cat primary visual cortex. Eur J Neurosci 16:1620–1626.

Van der Gucht E, Clerens S, Jacobs S, Arckens L. 2005. Light-induced Fos expression in phosphate-activated glutaminase- and neurofilament protein-immunoreactive neurons in cat primary visual cortex. Brain Res 1035:60–66.

Wang X, Zhang G, Sun M, Geller AI. 2001. General strategy for constructing large HSV-1 plasmid vectors that co-express multiple genes. Biotechniques 31:204–212.

Warburton EC, Glover CP, Massey PV, Wan H, Johnson B, Bienemann A, Deuschle U, Kew JN, Aggleton JP, Bashir ZI, Uney J, Brown MW. 2005. cAMP responsive element-binding protein phosphorylation is necessary for perirhinal long-term potentiation and recognition memory. J Neurosci 25:6296–6303.

Wayman GA, Lee YS, Tokumitsu H, Silva A, Soderling TR. 2008. Calmodulin-kinases: Modulators of neuronal development and plasticity. Neuron 59:914–931.

Weeber EJ, Atkins CM, Selcher JC, Varga AW, Mirnikjoo B, Paylor R, Leitges M, Sweatt JD. 2000. A role for the beta isoform of protein kinase C in fear conditioning. J Neurosci 20:5906–5914.

Winters BD, Forwood SE, Cowell RA, Saksida LM, Bussey TJ. 2004. Double dissociation between the effects of peri-postrhinal cortex and hippocampal lesions on tests of object recognition and spatial memory: Heterogeneity of function within the temporal lobe. J Neurosci 24:5901–5908.

Yuan Q, Harley CW, Darby-King A, Neve RL, McLean JH. 2003. Early odor preference learning in the rat: Bidirectional effects of cAMP response element-binding protein (CREB) and mutant CREB support a causal role for phosphorylated CREB. J Neurosci 23:4760–4765.

Zhang G, Cao H, Kong L, O'Brien J, Baughns A, Jan M, Zhao H, Wang X, Lu X, Cook RG, Geller AI. 2010a. Identified circuit in rat postrhinal cortex encodes essential information for performing specific visual shape discriminations. Proc Natl Acad Sci USA 107:14478–14483.

Zhang G, Cao H, Li X, Zhao H, Geller AI. 2010b. Genetic labeling of both the axons of transduced, glutamatergic neurons in rat postrhinal cortex and their postsynaptic neurons in other neocortical areas by Herpes Simplex Virus vectors that coexpress an axon-targeted ß-galactosidase and wheat germ agglutinin from a vesicular glutamate transporter-1 promoter. Brain Res 1361:1–11.

Zhang G, Wang X, Kong L, Lu X, Lee B, Liu M, Sun M, Franklin C, Cook RG, Geller AI. 2005. Genetic enhancement of visual learning by activation of protein kinase C pathways in small groups of rat cortical neurons. J Neurosci 25:8468–8481.

Zhang G, Wang X, Yang T, Sun M, Zhang W, Wang Y, Geller AI. 2000. A tyrosine hydroxylase--Neurofilament chimeric promoter enhances long-term expression in rat forebrain neurons from helper virus-free HSV-1 vectors. Mol Brain Res 84:17–31.